SACLANTCEN MEMORANDUM
serial no.: SM-354

SACLANT UNDERSEA
RESEARCH CENTRE
MEMORANDUM

SCINTILLATION INSTRUMENT FOR REMOTE ENVIRONMENTAL ANALYSIS (SIREN)

D. Di Iorio, D.M. Farmer, W. Cartier, X. Geng

February 1999

Report no. changed (Mar 2006): SM-354-UU

SACLANT Undersea Research Centre
Viale San Bartolomeo 400
19138 San Bartolomeo (SP), Italy

tel: +39-0187-5271
fax: +39-0187-524.600

e-mail: library@saclantc.nato.int

NORTH ATLANTIC TREATY ORGANIZATION

Scintillation Instrument for Remote Environmental Analysis (SIREN)

D. Di Iorio, D. M. Farmer,
W. Cartier, X. Geng

The content of this document pertains to work performed under Project 033-5 of the SACLANTCEN Programme of Work. The document has been approved for release by The Director, SACLANTCEN.

Jan L. Spoelstra
Director

intentionally blank page

Scintillation Instrument for Remote Environmental Analysis (SIREN)

D. Di Iorio, D. M. Farmer*, W. Cartier+, X. Geng#

Executive Summary:

Instrumentation for high frequency acoustic propagation in coastal and shallow water environments requires the capability of multipath separation (and hence large bandwidths), high transmission rates, large signal to noise ratio and precise timing information for accurate phase measurements. SIREN (scintillation instrument for environmental analysis) can be used to study coastal ocean processes and the effects of the water column variability on acoustic propagation practically on a continuous basis is described. For mine-counter-measures during which there is a need to understand the effect of ocean variability on high resolution sonar response, particularly synthetic aperture sonars, the modular design of the instrument is such that a variety of configurations can be implemented.

* Research Scientist, Fisheries and Oceans Canada, Institute of Ocean Sciences, 9860 West Saanich Rd., Sidney, B.C., V8L 4B2, Canada
+ Engineering Physicist, ASL Environmental Sciences Ltd., 1986 Mills Rd., Sidney, B.C., V8L 5Y3, Canada
# Software Engineer, Fisheries and Oceans Canada, Institute of Ocean Sciences, 9860 West Saanich Rd., Sidney, BC., V8L 4B2, Canada

intentionally blank page

Scintillation Instrument for Remote Environmental Analysis (SIREN)

D. Di Iorio, D. M. Farmer, W. Cartier,
X. Geng

Abstract:

A high frequency acoustic propagation instrument which was developed to study ocean variability in the Strait of Istanbul (Bosporus) is described. The scintillation instrument for remote environmental analysis (SIREN) was designed in modular form taking advantage of modern digital signal processing hardware and software so that data can be acquired continuously at relatively high transmission rates and in reciprocal directions. The overall design and operation of the system proved to be very good except for a digitization triggering problem, caused by a distorted trigger signal as a result of the long underwater cables used. This problem affected the measurement of the acoustic phase and hence the accuracy of ocean parameters for turbulence measurements. The amplitude however can be used as a measure of the total scattered signal due to turbulent sound speed and current velocity. The mean travel time gives mean ocean variability. The experimental period is summarized and the data processing techniques are described.

Contents

List of Figures

List of Tables

1

Introduction

It has long been recognised that natural variability in the environment through which an electromagnetic or acoustic wave is travelling modifies the signal in ways that open up possibilities for recovering information about the medium. Our application of acoustical scintillation to ocean measurement has its origin in the interpretation of modulation of radio signals from distant objects by the interplanetary plasma. Variability in the plasma density in space, or variability in temperature and salinity for acoustical propagation in the ocean, distorts the spherically spreading phase fronts which result in amplitude and phase fluctuations (scintillation). For acoustical propagation in the coastal environment, small scale fluctuations in the flow velocity can have equal or greater effect.

As the fine structure variability in the medium has a natural coherence time, it will be transported by the current, with the scattered pattern. Detection of pattern motion is the essential concept exploited in acoustical scintillation. The basic idea was successfully used with radio telescopes to measure wind using optical and microwave scatter (Ishimaru, 1978). More recently it has been demonstrated using acoustical propagation in the ocean and is a key principle in systems we describe here for measurement of coastal currents (Farmer and Clifford, 1986; Farmer *et al.*, 1985).

An important feature of this approach is that the measurement is of the flow component perpendicular to the acoustic path, which for many practical applications is of greatest interest. Using the well established principle of reciprocal propagation however, allows this approach to be extended to measurement of flow along the path, resulting in measurement of two orthogonal components of the current vector (Di Iorio and Farmer, 1998). These measurements are path averaged, which may also be an advantage if water transport rather than the detailed flow structure is the measurement of interest. Acoustical paths may also be set up to operate at several depths simultaneously allowing vertical profiles to be acquired. However, although forward scatter measurements are primarily path averaged, it is also possible to exploit the translation of coherent structure through the acoustical path so as to achieve measurement as a function of path position using spatial aperture filtering (Crawford *et al.*, 1990; Farmer and Crawford, 1991).

Analysis of the signals can go well beyond a simple measurement of flow speed, and has included detection of turbulent velocity fluctuations (Di Iorio and Farmer,

1994; Menemenlis, 1994), turbulent anisotropy (Di Iorio and Farmer, 1996), vorticity (Menemenlis and Farmer, 1992) and fish migration (Curran *et al.*, 1994; Ye and Farmer, 1996; Ye *et al.*, 1996). The application of these techniques has now become well established as a result of a number of studies in coastal channels, rivers and beneath the Arctic ice cover. In general, the application has involved the use of high frequencies and correspondingly short paths of a few kilometres or less. Wholly refracted paths are desirable, although surface and bottom interacting signals may also contain interesting information; separation of multiple paths usually demands the application of larger bandwidths and some care in choosing an appropriate site.

A particularly interesting application is in the measurement of bi-directional flow in a strait. In section 2 we describe an implementation for measurement of flow in the Strait of Istanbul (Bosporus), which is part of the Turkish Straits connecting the Black Sea to the Sea of Marmara (Ünlüata *et al.*, 1990). The watershed for large areas of central and eastern Europe drains into the Black Sea producing a brackish layer that moves along the surface through the Strait. Continuity of salt requires that a counter current of saline water enter beneath. The rate at which these two layers exchange is a problem of classical origins (Marsigli, 1681) having important implications for long term changes in water properties as well as more practical issues such as navigation and pollution management.

Sections 3 and 4 give a detailed description of the acoustical scintillation system and section 5 shows sample data collected from the Strait of Istanbul (Bosporus) together with a preliminary analysis.

2 Implementation

Acoustical scintillation has been employed in the measurement of flows in coastal straits (Farmer *et al.*, 1985; Di Iorio and Farmer, 1994, 1998), rivers (Curran *et al.*, 1994) and beneath the arctic ice cover (Menemenlis and Farmer, 1992). The implementation of such systems has evolved steadily as the technology for real time processing, data acquisition and data storage has improved. In order to illustrate the most recent state of this development we describe an acoustic scintillation system designed for installation in the Strait of Istanbul (Bosporus).

The scintillation instrument for remote environmental analysis (SIREN) is an acoustic forward scatter system capable of fully synchronous reciprocal transmission. The system is deployed in the Strait of Istanbul (Bosporus) between Anadolu Hisari, on the east side, and Rumeli Hisari, on the west side (Figure 1). The primary objective of the instrument is to measure water exchange through the Strait between the Sea of Marmara and the Black Sea in addition to measuring acoustical properties. A block diagram of the system is shown in Figure 2(a) and the transducer geometry is shown in Figure 2(b).

Acoustical propagation across the Strait of Istanbul (Bosporus) is sensitive to the vertical sound speed structure. Seasonal variations and changing meteorological conditions are known to modify the exchange flow and hence the vertical structure. For example an excessive sea level difference between the Black and Marmara Seas as a result of an atmospheric pressure gradient or strong northeasterly winds can halt the Mediterranean undercurrent thus causing a change in the interface depth or depth of strongest sound speed gradient. Also, seasonal cooling and heating will change the temperature of the surface Black Sea water to 4 and 24 ^oC respectively thus creating a strong sound speed channel at mid depth during the summer season.

The scintillation paths of primary interest are wholly refracted and their geometry will vary with the changing pattern of sound speed profile. Figure 3 is an example of the sound speed profile taken in July 1997 together with the eigenrays which connect the transmitters and receivers on opposite sides of the channel. In this example, measurements show a time separation between the direct path and wholly refracted path ranging between 40 and 3500 μs for the upper layer and 660 μs for the lower layer.

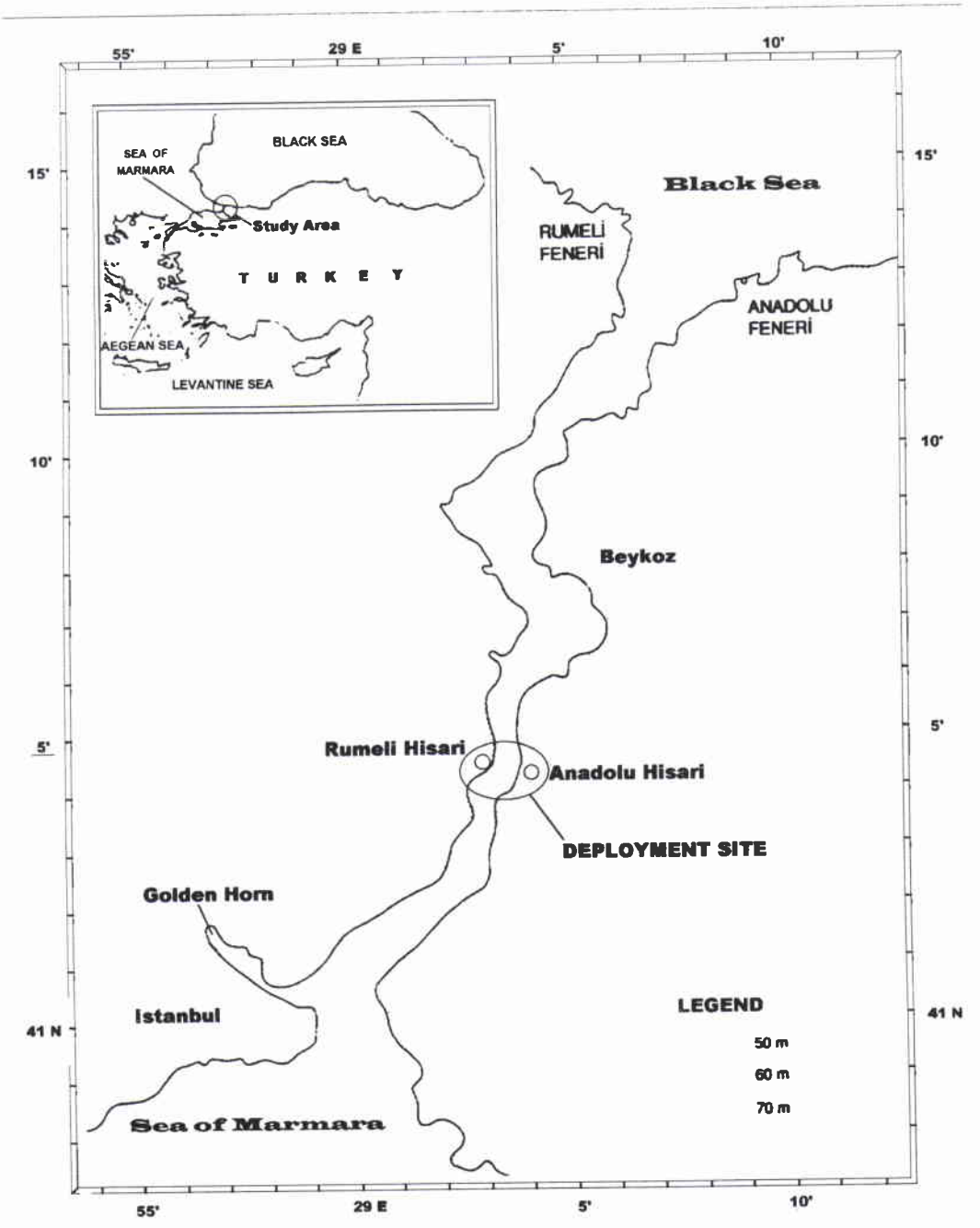

Figure 1 *Deployment site in the Strait of Istanbul (Bosporus). The acoustical system is deployed on both sides of the strait.*

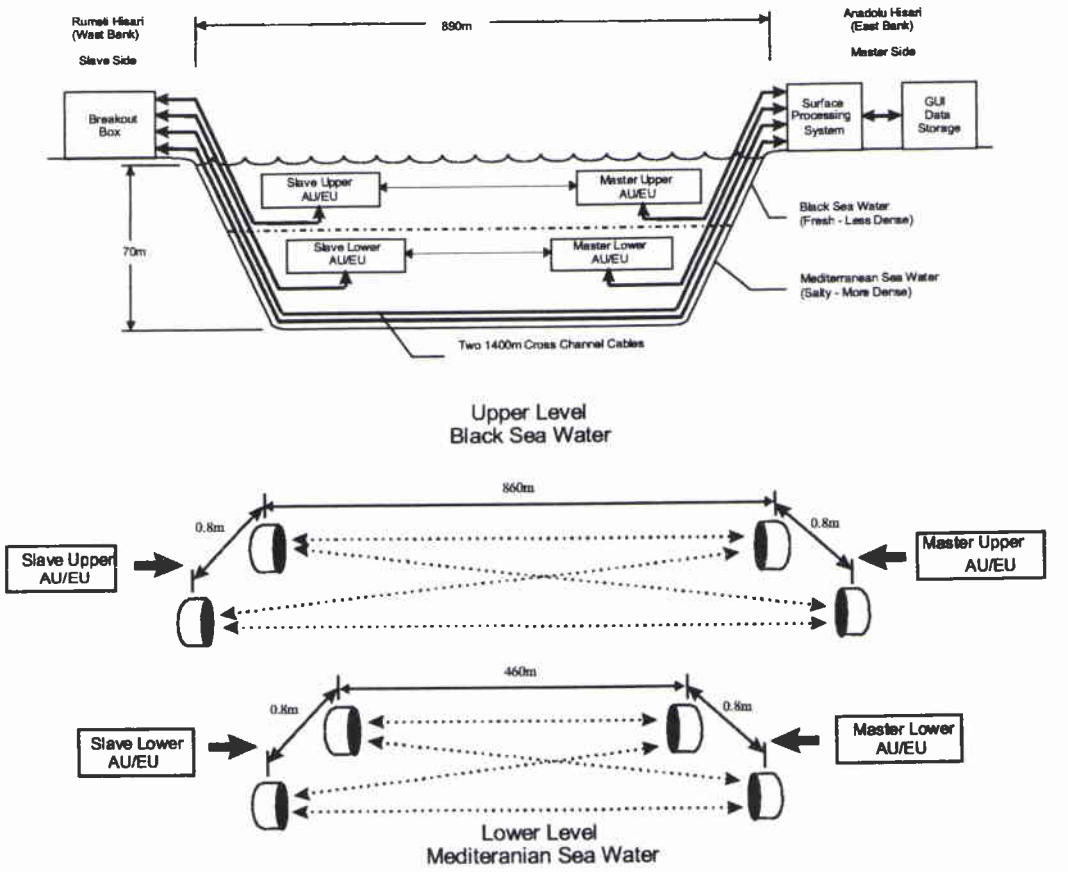

Figure 2 *(upper) Schematic representation of the SIREN system in the Strait of Istanbul (Bosporus). (lower) SIREN transducer geometry.*

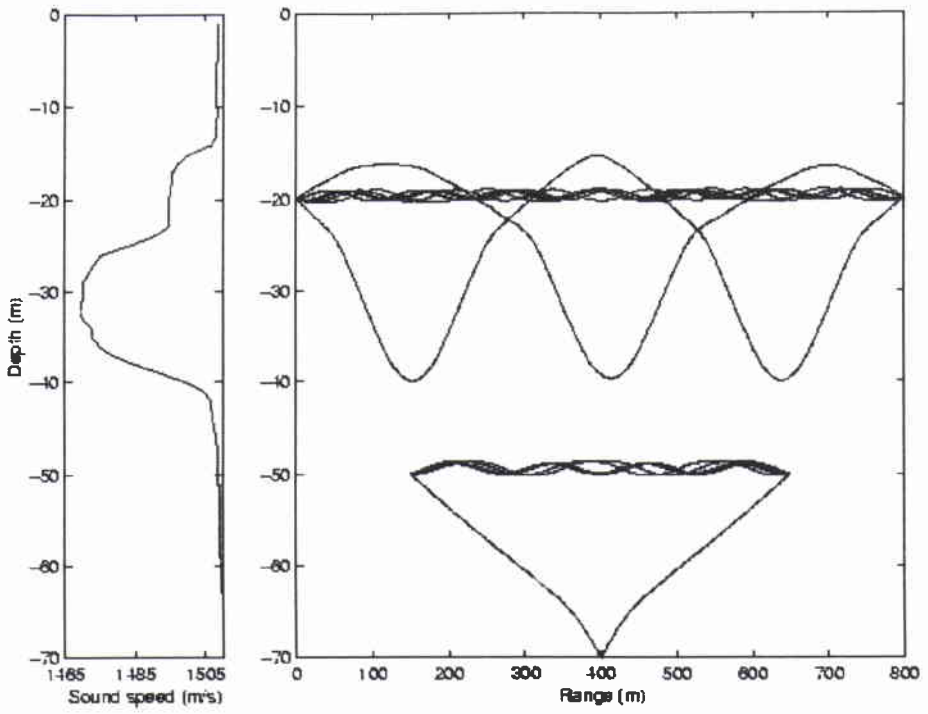

Figure 3 *Sound speed profile taken in July 1997 together with eigenrays which connect transducers on either side of the channel.*

3

Engineering Design Approach

The present system differs to previous acoustical scintillation systems (Farmer *et al.*, 1985; Di Iorio and Farmer, 1994, 1998; Menemenlis and Farmer, 1992) in its modular structure, flexible software control and the implementation of modern processing technology. Digital signal processing (DSP) hardware and processing techniques, embedded controller and distributed computing technology, lead to more flexible software based modular design. This system is capable of transmitting and receiving synchronous reciprocal acoustical signals at high pulse repetition rates. Sonar signals received from multiple transceiver sites are processed in real time and stored for subsequent processing. From this raw data, measurements are obtained of the path averaged properties including turbulence, sound speed structure and two components of flow speed at a given depth.

As our primary interest is in the analysis of wholly refracted paths, sufficient time resolution is needed to separate arrivals from different paths while maintaining a sufficiently large signal-to-noise ratio (SNR). This is most effectively handled with spread spectrum techniques. For example a 180^o phase-modulated 127 bit m-sequence provides a processing gain of

$$20 \log \sqrt{n} \approx 21 \text{dB}, \tag{1}$$

where n=127 is the number of m-sequence code bits (Dixon, 1984). This coded broadband transmission provides a temporal resolution of

$$2\tau_p = 2f_{SBW}^{-1}, \tag{2}$$

where τ_p is the bit width of the m-sequence and f_{SBW} is the signal bandwidth.

The coded signal consists of a binary modulation of a 50.813 kHz carrier by a 127 bit pseudo random code which is a maximal linear sequence. The binary transitions are keyed as 180^o phase shifts of the carrier. Figure 4 shows a sample code for a 7-bit shift register M(7,1) with its autocorrelation function. The correlation peak is triangular with height $2^7 - 1$ and width 2 bits at zero delay. On each side of the peak, there are correlation sidelobes. Correlation sidelobes from multipaths may interfere with the main peak. The amount of interference depends on relative amplitude and time delay between each multipath. The effects of sidelobe interference may however be eliminated or minimized by adding guard sequences. Figure 4 shows the matched filter output when a single code is correlated with three consecutive codes. The SNR is increased as a result.

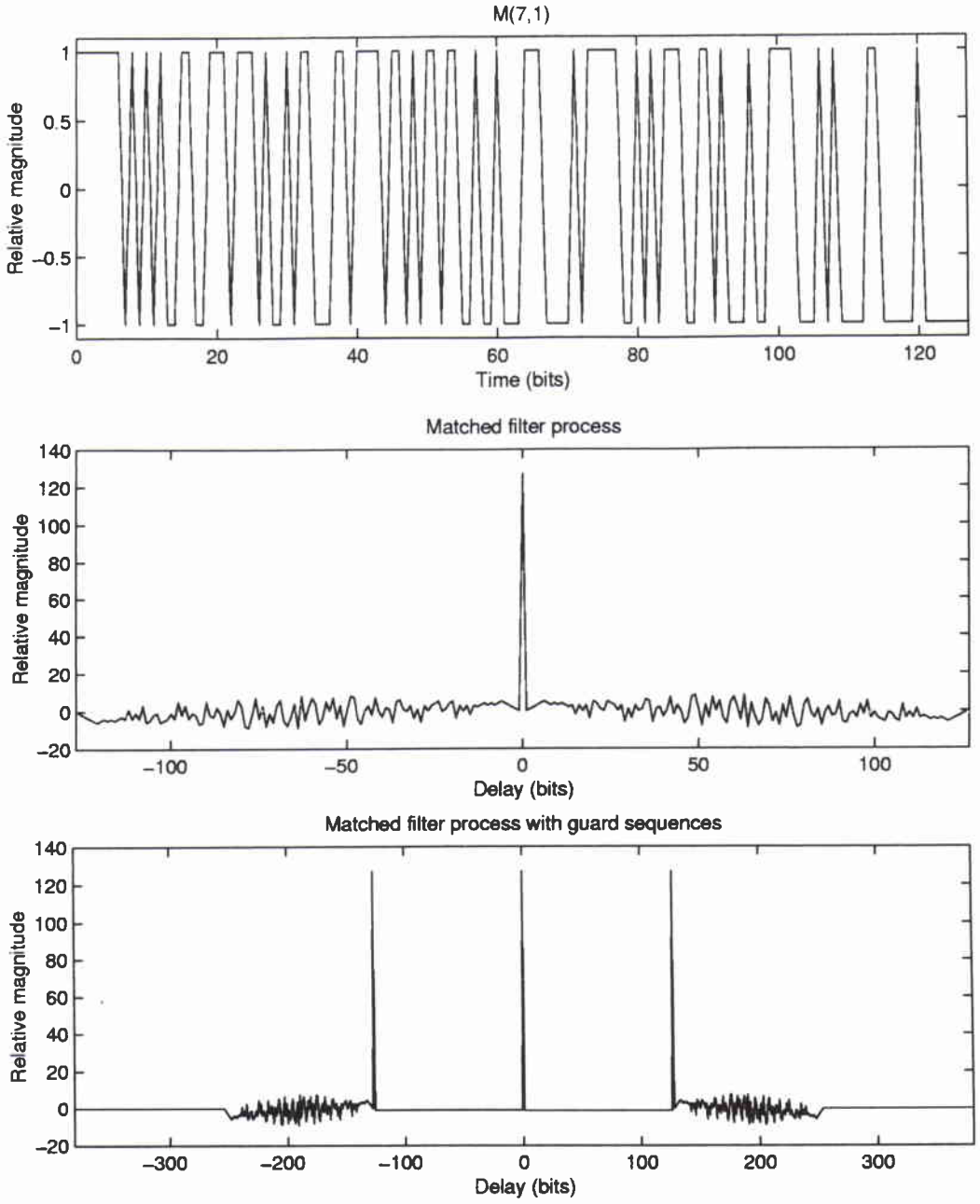

Figure 4 *Pseudo random noise sequence generated by a 7-bit shift register. The autocorrelation function exhibits a triangular peak at zero lag. Correlation side lobes are eliminated by using guard sequences.*

For implementation in the Strait of Istanbul (Bosporus) the 50.813 kHz transducers have a 15% bandwidth corresponding to 7.6 kHz. The signal bandwidth however is based on the bit width of the m-sequence code. A bit width of 6 cycles/bit was normally used, thus giving a signal bandwidth of 8.333 kHz. The system is therefore able to resolve multipaths separated in time by,

$$2f_{SBW}^{-1} \approx 240\mu s \tag{3}$$

which corresponds to a path length difference in sea water of approximately 0.4 m. There are two effects from having the signal bandwidth slightly larger than the transducer bandwidth. First, the signal to noise ratio (SNR) is slightly decreased and second, the correlation peak is broadened by approximately 10%. These effects are minor compared to the gain received by being able to separate multipaths by 240 μs.

Figure 5(a) shows two primary sub-systems comprising the basic data acquisition module. These include surface and sub-surface units connected by cable. The sub-surface system includes three major components: a remote positioning system for orienting narrow beam transducers in the appropriate direction, an environmental unit containing conductivity-temperature-depth (CTD) sensors and an acoustic unit. The acoustic unit includes an analogue transceiver section, 203.252 kHz 16 bit analogue-to-digital (A/D) and digital-to-analogue (D/A) converters, real time DSP electronics, a host processor and high speed serial data transmission circuitry. The surface unit also includes three major components: a data acquisition system that distributes timing signals to the sub-surface acoustic unit and receives processed data from the sub-surface unit, a graphic user interface through which a user interacts with the system and data storage device. These three components are connected through a 10 Mbit s^{-1} Ethernet local area network (LAN) system. This design has the advantage of being flexible in different deployment strategies.

Using the sub-systems shown in Figure 5(a), an additional sub-surface system is added yielding the design shown in Figure 5(b). This represents a single level acoustic forward scatter scintillation data acquisition system capable of synchronous transmissions in both directions. Assuming that each side has two hydrophones with a dedicated channel for each at a given level, gives a minimum of four acoustic paths in each direction, giving a total of eight paths on a single level. Refractive effects in the water column together with surface and bottom scatter will increase this number. Two sub-surface systems are added for the deeper transducers. The modular nature of the design allows straightforward expansion to a larger number of transducers.

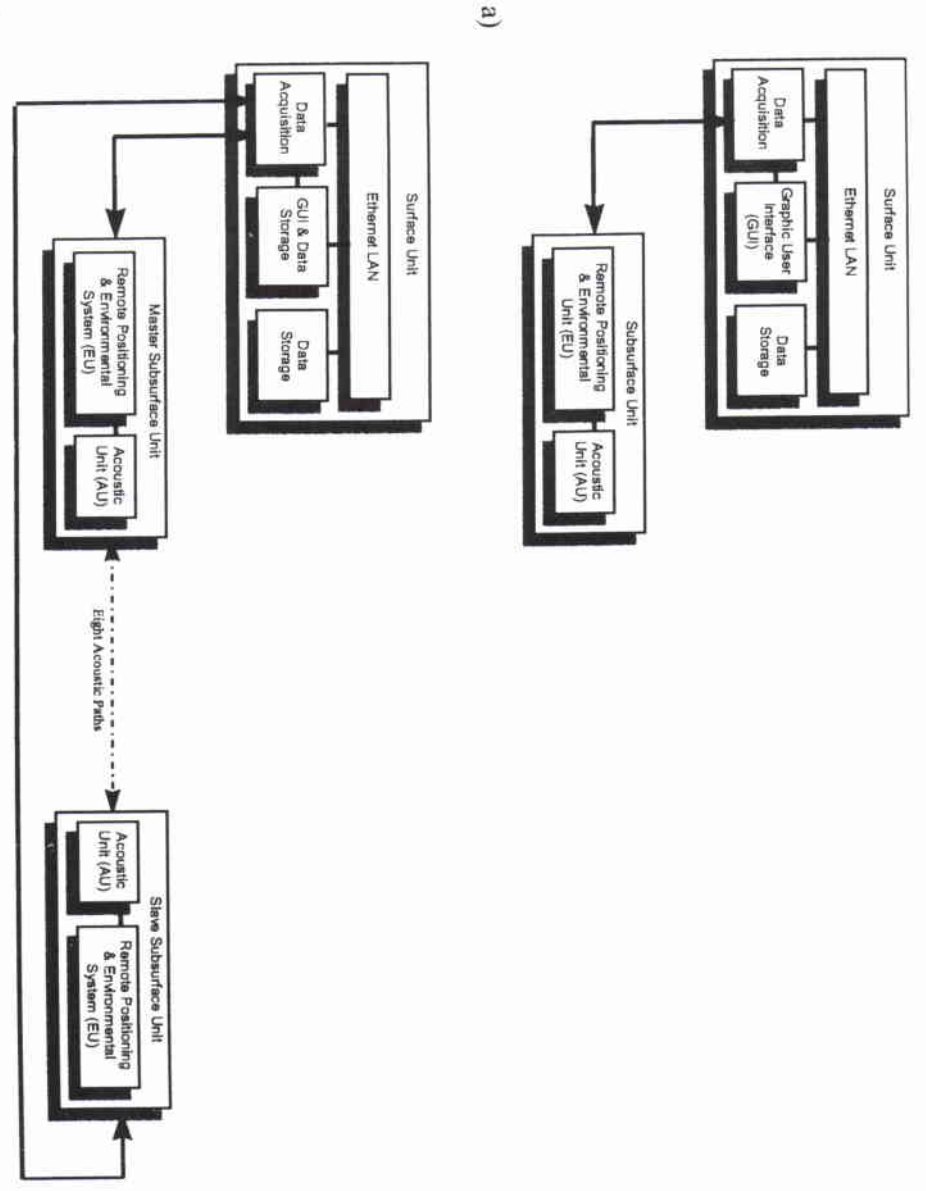

Figure 5 *Block diagram showing (a) primary sub-systems of SIREN and (b) simple single level acoustic forward scatter data acquisition system.*

4

System Description

SIREN is capable of full forward and reciprocal transmissions at pulse repetition rates greater than 20 Hz for simple pulses, approximately 8 Hz for 127 bit broadband spread spectrum simultaneous transmissions and approximately 4 Hz 127 bit broadband spread spectrum consecutive transmissions. It employs the Texas Instruments TMS320C32 DSP for data acquisition and real-time signal processing. At these high repetition rates, several pulses are in the water at the same time. The system is designed so as to ensure that pulse arrivals occur between successive transmissions, as it is not possible to receive and transmit from the same transducer.

System timing, including a 203.252 kHz master clock and ping rate trigger signals are synchronous and generated by the master controller as shown in Figure 6 which together with power is distributed *via* six cables (Figure 2). Two 1400 m cross channel cables originate at the master station, on the east side of the Strait of Istanbul (Bosporus) at Anadolu Hisari, and terminate at a breakout box on the west side of the Strait at Rumeli Hisari. Two additional cables of length 200 m and 400 m, extending from the breakout box, run to the upper and lower slave sub-surface units respectively. Two additional cables extend from the master surface unit and run to the upper and lower master sub-surface units. The cables are armoured and consist of five duplex shielded twisted pairs and four power conductors.

System control inputs, real-time display of system parameters and data are handled by an operator through a graphic user interface. System parameters are sent to the master data acquisition and control unit where the commands are sent to the appropriate acoustic, remote positioning, and environmental units (Figures 2, 6, 7 and 8). Data are stored on a tape with a capacity of 4.0 Gbytes sufficient to accommodate continuous raw data for approximately one week.

Due to the depth and strong currents at the site, which preclude use of divers for deployment, a remote positioning system supports each pair of transducers. A pan and tilt unit with orientation and azimuth sensors allow an operator to control their alignment. Each sub-surface system has full conductivity, temperature and depth measurement capability.

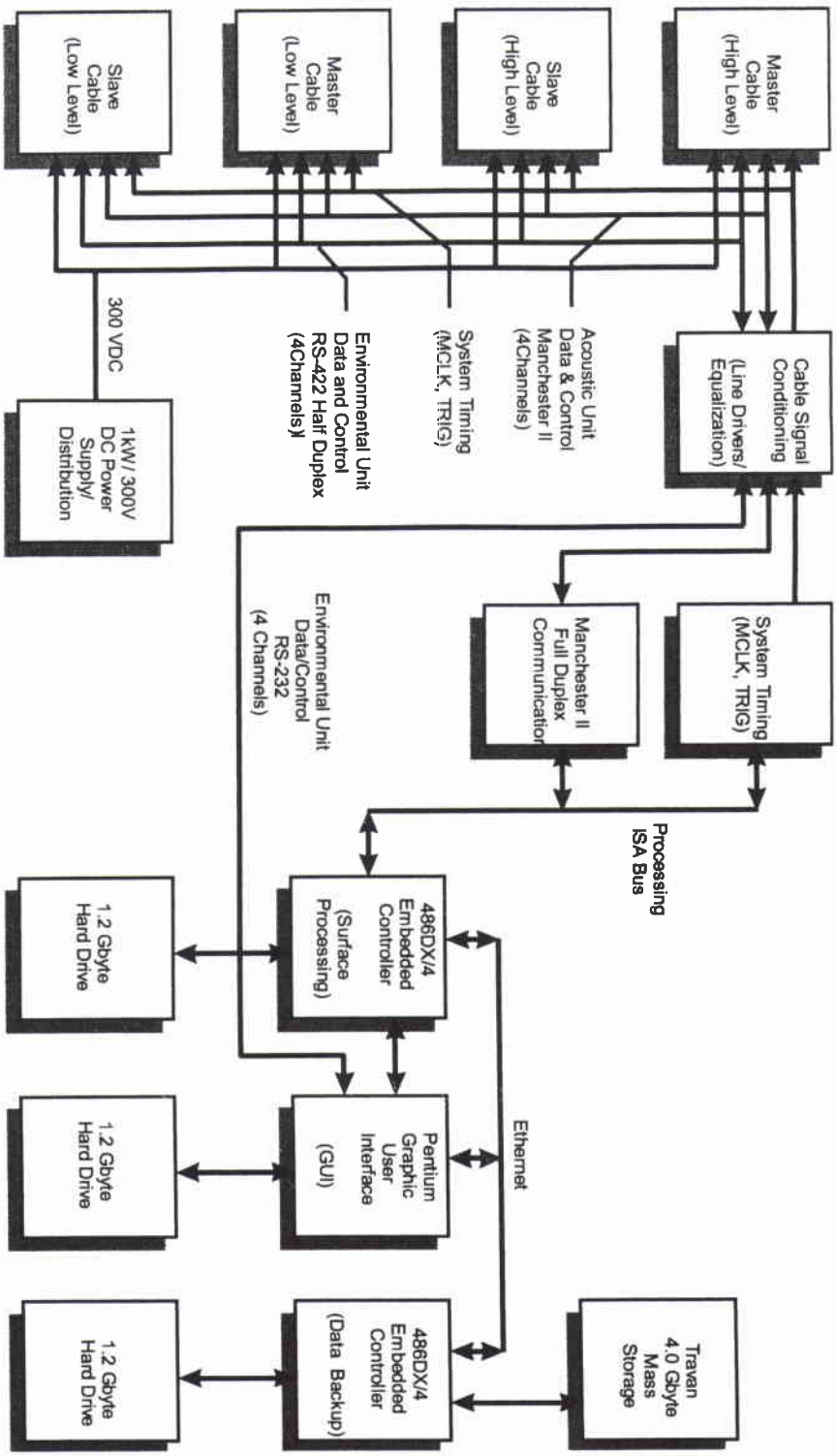

Figure 6 *Block diagram showing master data acquisition, processing, control, display and storage systems.*

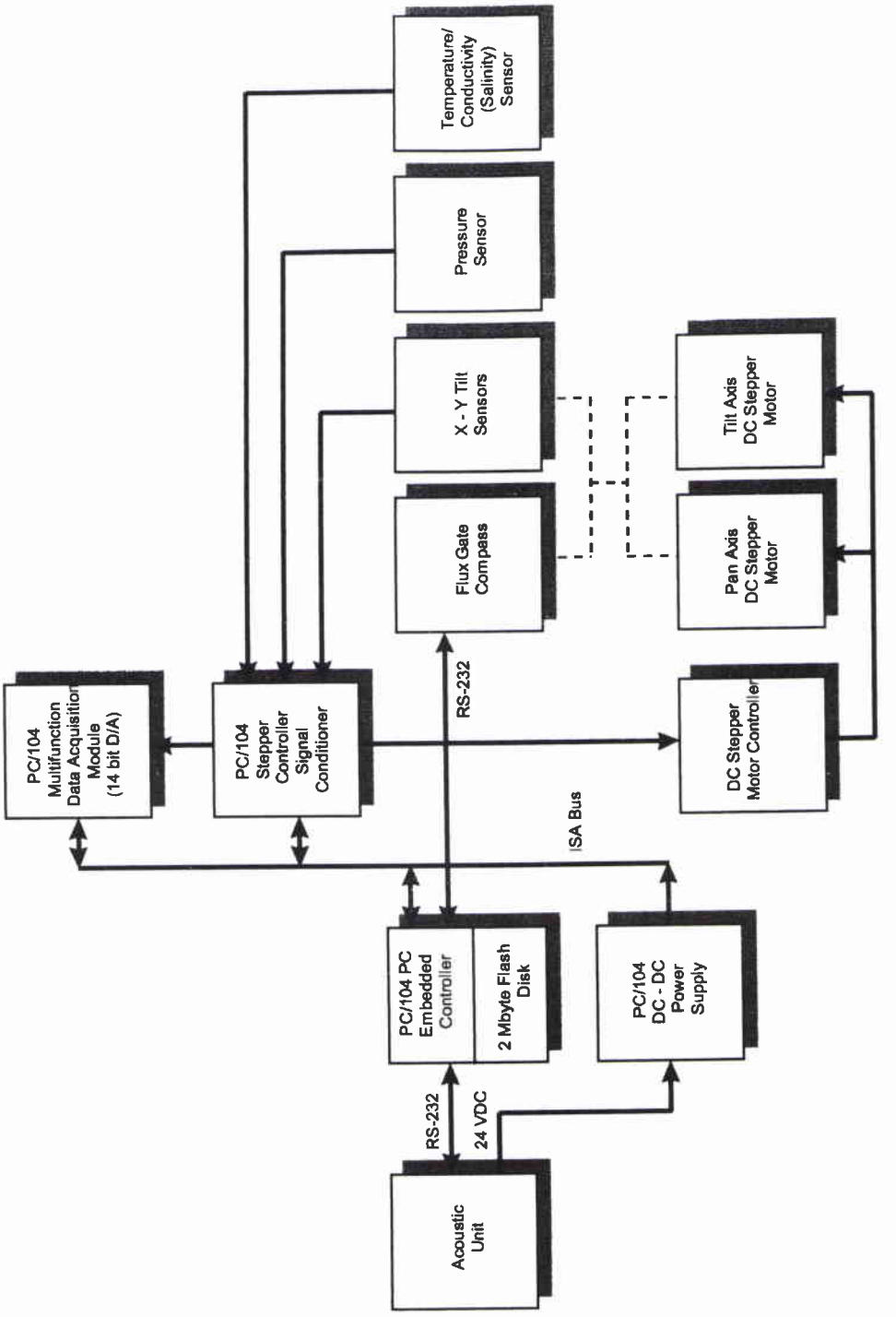

Figure 7 *Block diagram showing environmental unit with the remote positioning system.*

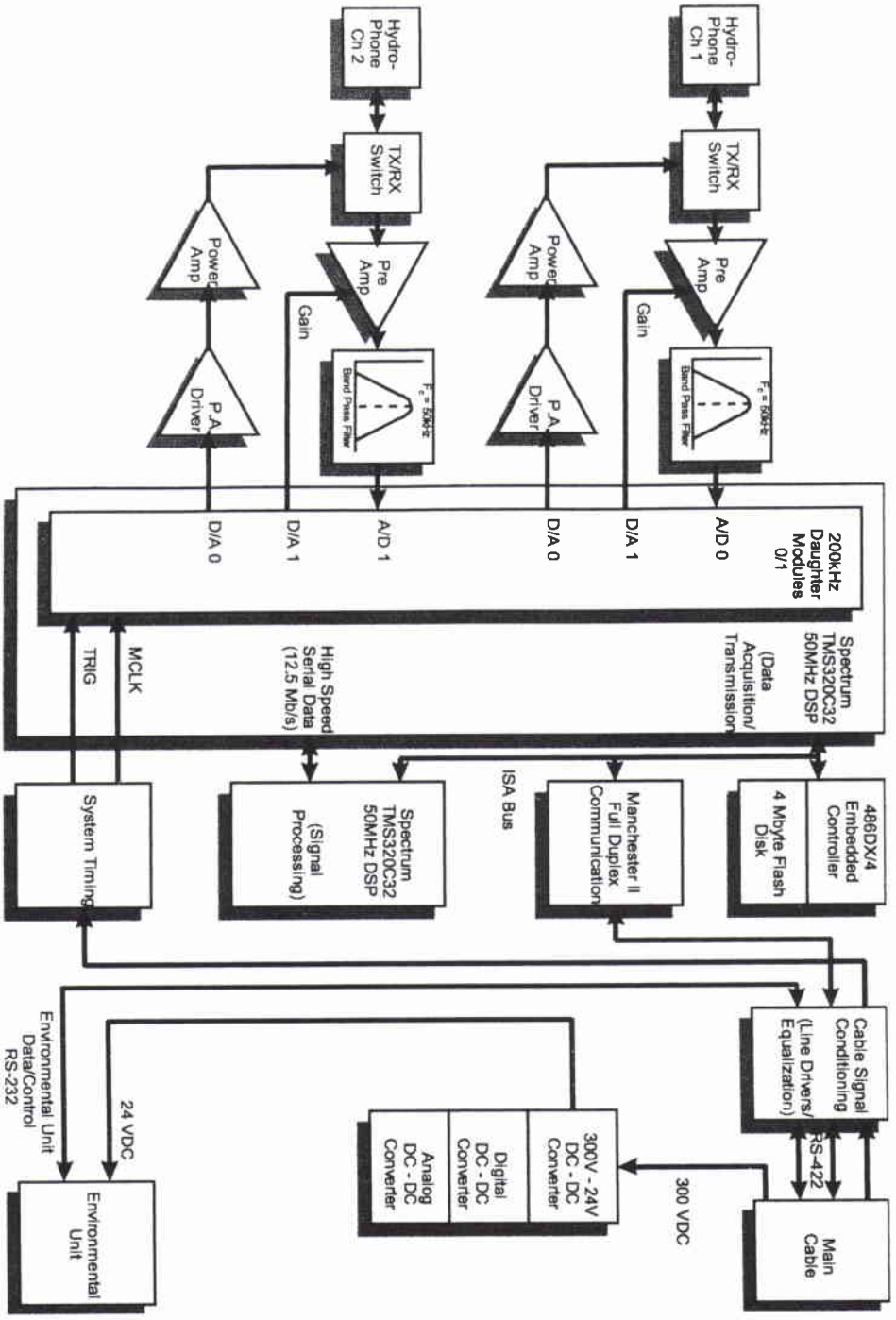

Figure 8 *Acoustic unit block diagram.*

4.1 Simultaneous transmissions

The scintillation data is gathered on each level by the acoustic units (Figure 8). In this scheme, upon reception of a timing trigger (which is the ping rate clock) the data acquisition/transmission (TxRx) DSP outputs digital data (which is stored in memory) to the D/A converter at the master clock (MCLK) rate of 203.252 kHz. This digital data consists of,

$$127\frac{bits}{code} * 6\frac{cycles}{bit} * 4\frac{samples}{cycle} = 3048 samples/code \tag{4}$$

where the code is an M(7,0) sequence for one transmitting hydrophone and an M(7,1) sequence for the other transmitting hydrophone. Three codes consisting of 3*3048=9144 quadrature samples are modulated by $\sin(2\pi ft)$ and sent to the D/A and output to each transmitter each having a different m-sequence code. Transmissions occur at the same time. Three codes are transmitted as the first and third code act as guard sequences to the second code thus increasing the SNR when matched filter processing is carried out (correlation side lobes cancel).

The data processing (PROC) DSP has two templates of 381 complex samples zero padded to 2048 complex samples and stored in memory. The real part is the quadrature component and the imaginary part the inphase which are zero. Each template represents the two different m-sequence codes. The complex fast Fourier transform (FFT) of these templates are also stored in memory. These templates have a sampling rate of 3 samples/bit.

Once the transmissions occur, A/D sampling occurs for each hydrophone at the master clock rate of 203.252 kHz. This sampling rate corresponds to 4 samples/cycle where a sample is separated by 90^o giving inphase and quadrature sampling. In order to minimize the data collected, a delay based on the propagation time and ping rate is calculated and converted to total samples. These samples are discarded and 10% in excess of the total signal width is collected giving 3*3048*1.1=10058 samples (5029 quadrature and 5029 inphase samples). The inphase and quadrature components are then subsampled by a factor 4 and zero padded to 2048. The data from both hydrophones are transferred to the PROC DSP for real-time processing. This reduced data has a final sampling rate of 3 samples/bit as does the template.

As each acoustic unit transmits on each of two hydrophones simultaneously a different code, the PROC DSP must perform two independent correlations for each receiving hydrophone. This is carried out by FFT methods. The transmission from each hydrophone on the opposite side of the channel can be distinguished upon reception of the combined signals. At each receiving hydrophone the signal correlated with M(7,0) sequence gives transmitter 1 data and the signal correlated with M(7,1) sequence gives transmitter 2 data. These pseudo random noise codes are

such that correlating M(7,0) with M(7,1) gives noise for all delays and this noise will be introduced into the final signal output.

The resulting correlated inphase and quadrature data is sent to the embedded processor (the sub-surface computer) for windowing to select the desired transmissions. This windowed data is sent to the communication card where it is transmitted as a 400 kbaud Manchester II encoded serial digital data stream up the cable to the master data acquisition system on the surface for display and storage. This reduces the amount of data in order to accommodate the reduced bandwidth over the length of the cable. Master transmissions are received by the slave and then sent via the 1.6 km cable and the 1.8 km cable for the upper and lower layer units respectively.

The data stored consist of 8 acoustic paths with each path having windowed quadrature and inphase components. Four of the paths correspond to propagation from the slave to master and the other four from the master to slave. The windowed data typically consists of 150 samples of inphase and quadrature values.

4.2 Consecutive transmissions

This mode is similar to the simultaneous transmission scheme except that the transmissions are carried out consecutively. In this scheme, upon reception of the ping rate trigger, the TxRx DSP outputs digital data (which is stored in memory) to the D/A converter at the MCLK rate of 203.252 kHz. This digital data consists of 3048 samples of the M(7,0) sequence. Four codes consisting of 4*3048=12192 quadrature samples are modulated by $\sin(2\pi ft)$ and are sent to the D/A. For transmitter 1 the signal is multiplied by 1 volt for the first two codes and 0 Volts for the last two codes. For transmitter 2 the signal is multiplied by 0 Volt for the first two codes and 1 Volt for the last two codes. The signal output occurs simultaneously but the transmissions occur consecutively. Four codes are transmitted into the water as the first and third code are guard sequences to the second code which is the signal from transmitter 1 and the second and fourth code act as guard sequences to the third code which is the signal from transmitter 2.

The PROC DSP has the m-sequence template of 381 complex samples zero padded to 2048 complex samples stored in memory. The complex FFT of this template is also stored in memory.

The sampling scheme is carried out as for the simultaneous transmission scheme except that 10% of the total signal width is collected giving 4*3048*1.1=13412 samples. The 6706 samples of quadrature and inphase are subsampled by a factor of 4 and zero padded to 2048 samples. These data are transferred to the PROC DSP for real-time processing.

A single correlation by FFT methods for each receiving hydrophone is carried out. The second and third correlation peak correspond to the transmissions from transmitter 1 and 2 respectively. The correlation data for each hydrophone are sent to the sub-surface computer for windowing and these data are sent up the cable to the surface computer for data display and storage.

5

Experimental Summary

The deployment of the SIREN system in the Strait of Istanbul (Bosporus) presented many challenges and the events are summarized here. This joint project involved SACLANTCEN, the Institute of Ocean Sciences (IOS) and the Department of Navigation, Hydrography and Oceanography (DNHO) of the Turkish Navy.

During the period of July 11 to August 9, 1997, the SIREN system was successfully deployed despite the many challenges. The deployment was quite involved, requiring cables to be laid across the Strait between Anadolu Hisari and Rumeli Hisari, followed by four tripod systems with each having their own cable attached to shore. Given the strong currents and wind in the strait, it proved necessary to maneuver the vessel with the aid of two tug boats. The Strait of Istanbul (Bosporus) is a major shipping strait and was closed to all large vessels during the deployment of the cross channel cables and tripods, thanks to the arrangements made by DNHO.

Table 1(a) shows the tripod depths, orientation and CTD measurements obtained from the environmental unit for August 1997. Sample acoustic data were collected for simultaneous transmissions, at a low ping rate. Due to lack of time the system could not be made fully operational.

In October 1997 it was discovered that the SL unit was not responding and hence the lower layer system was shut down. The upper layer system however was fully operational and data collection began. Initial parameter values are shown in Table 1(b). Table 2 gives a summary of the data collected and for which layer. The upper layer system continued to work until January 1998 when the tilt sensors indicated that the tripod was knocked over. A third trip was scheduled for August 1998 in order to recover all sub-surface tripods for maintenance and repairs.

Recovery and redeployment of the subsurface units posed many challenges because of the strong currents, wind and the heavy shipping traffic. The SU unit showed extensive mussel growth on the array and electronic cases. The acoustic unit pressure case was flooded. The SL environmental unit together with transducer array was torn off and lost possibly because a ship anchored onto the tripod, knocked it over, and ripped off the unit. The MU unit also had mussel growth. The ML unit had a cement anchor block entangled with the tripod. The environmental unit was torn off and hung by its cables. The environmental unit pressure case was flooded. From

(a)

Tripod	Heading (deg)	Pitch (deg)	Roll (deg)	Depth (m)	Cond. mMho/cm	Temp. (^oC)	Sal. (psu)	Sspd (m/s)
ML	272.4	0.87	-3.01	51.47	43.95	14.11	36.77	1506.8
MU	273.6	0.45	-6.47	24.49	25.03	16.11	18.77	1491.0
SL	89.2	0.75	-1.79	49.84	43.52	13.80	36.40	1504.9
SU	90.7	0.22	-5.52	18.98	23.83	13.77	18.85	1483.6

(b)

Tripod	Heading (deg)	Pitch (deg)	Roll (deg)	Depth (m)	Cond. mMho/cm	Temp. (^oC)	Sal. (psu)	Sspd (m/s)
MU	276.7	1.15	-4.22	24.77	17.99	17.66	12.57	1489.2
SU	92.5	1.39	-4.56	19.13	17.29	17.47	12.10	1488.0

Table 1 *(a) Tripod orientations and sensor indications for August 1997. The ML pressure sensor is a high resolution Paroscientific sensor giving the absolute pressure. For conversion to a depth measurement the standard pressure (14.98 psi) is subtracted. (b) Parameter values for the upper layer system for October 1997.*

Start time	End time	Layer	Transmission mode
August 6, 1997	August 7, 1997	both	simultaneous
October 1997	January 1998	upper	simultaneous
August 1998	December 1998	lower	consecutive

Table 2 *Table showing the times of data collection and for which layer.*

these four tripods two complete acoustic and environmental units were put together thus forming a complete layer system. The system was deployed in the lower layer as indicated in Table 2. The deployment configuration for August 1998 as measured from the environmental unit are shown in Table 3.

5.1 Data Processing

Annex A summarizes the format of the scintillation and environmental data files.

Tripod	Heading (deg)	Pitch (deg)	Roll (deg)	Depth (m)	Cond. mMho/cm	Temp. (^{o}C)	Sal. (psu)	Sspd (m/s)
ML	266.6	-0.63	-1.69	52.1	44.49	14.45	36.96	1508.1
SL	87.7	0.89	1.44	46.3	43.77	14.30	36.43	1506.1

Table 3 *Tripod orientations and sensor indications for August 1998. The ML pressure sensor is no longer the Paroscientific sensor.*

From the quadrature (Q) and inphase (I) components the amplitude of the acoustic signal as a function of travel time (t) is,

$$a(t) = \sqrt{Q(t)^2 + I(t)^2}, \tag{5}$$

and the phase is

$$\phi(t) = tan^{-1}\left(\frac{I(t)}{Q(t)}\right). \tag{6}$$

Figure 9(a) and (b) shows the relative amplitude as a function of arrival time and as a function of elapsed time for sample data taken in October 1997 and August 1998 respectively. For the October 1997 data, transmissions were simultaneous at a rate of 6.78 Hz over a propagation path length of approximately 700 m in the upper layer. The August 1998 data, consists of consecutive transmissions at a rate of 4.71 Hz over a propagation path length of approximately 500 m in the lower layer. For the simultaneous transmission case the amplitude image shown in Figure 9(a) shows horizontal bands which are a result of noise as the received signal is a superposition of the signals from the two transmitters. When consecutive transmissions were implemented in the August 1998 data the bands of correlation side lobe noise were removed.

The arrival pattern for the upper layer consists of a direct path followed closely by a wholly refracted arrival having greater amplitude. These are then followed by surface and bottom reflected paths. The arrival pattern for the lower layer consists of a direct path and a bottom reflected path. In order to calculate the amplitude ($A = a(T)$), phase ($\Phi = \phi(T)$) and arrival time (T) for a single acoustic path - the direct arrival, a maximum likelihood estimation algorithm is developed following Ehrenberg *et al.* (1978) and Di Iorio and Farmer (1993).

The mathematical model for the received signal $r(t)$ is,

$$r(t) = As(t - T) + n(t) \tag{7}$$

where t is the travel time. The signal $s(t)$ is known since it is the matched filter output determined by Menemenlis and Farmer (1992),

$$s(t - T) = \sum_{n=0}^{9} a_n \left(\frac{t - T}{\tau_p}\right)^{2n}, \tag{8}$$

where a_n are known coefficients and τ_p is the half-width of the correlation peak. The shape of this function is triangular with a rounded apex and can be seen in Figure 10 normalized to unit amplitude and zero arrival time.

The maximum likelihood estimation is derived as follows: minimize,

$$Q = \sum_t [r(t) - As(t - T)]^2, \tag{9}$$

$$= \sum_t r(t)^2 - 2\left[AC(T) - \frac{1}{2}A^2B(0)\right], \tag{10}$$

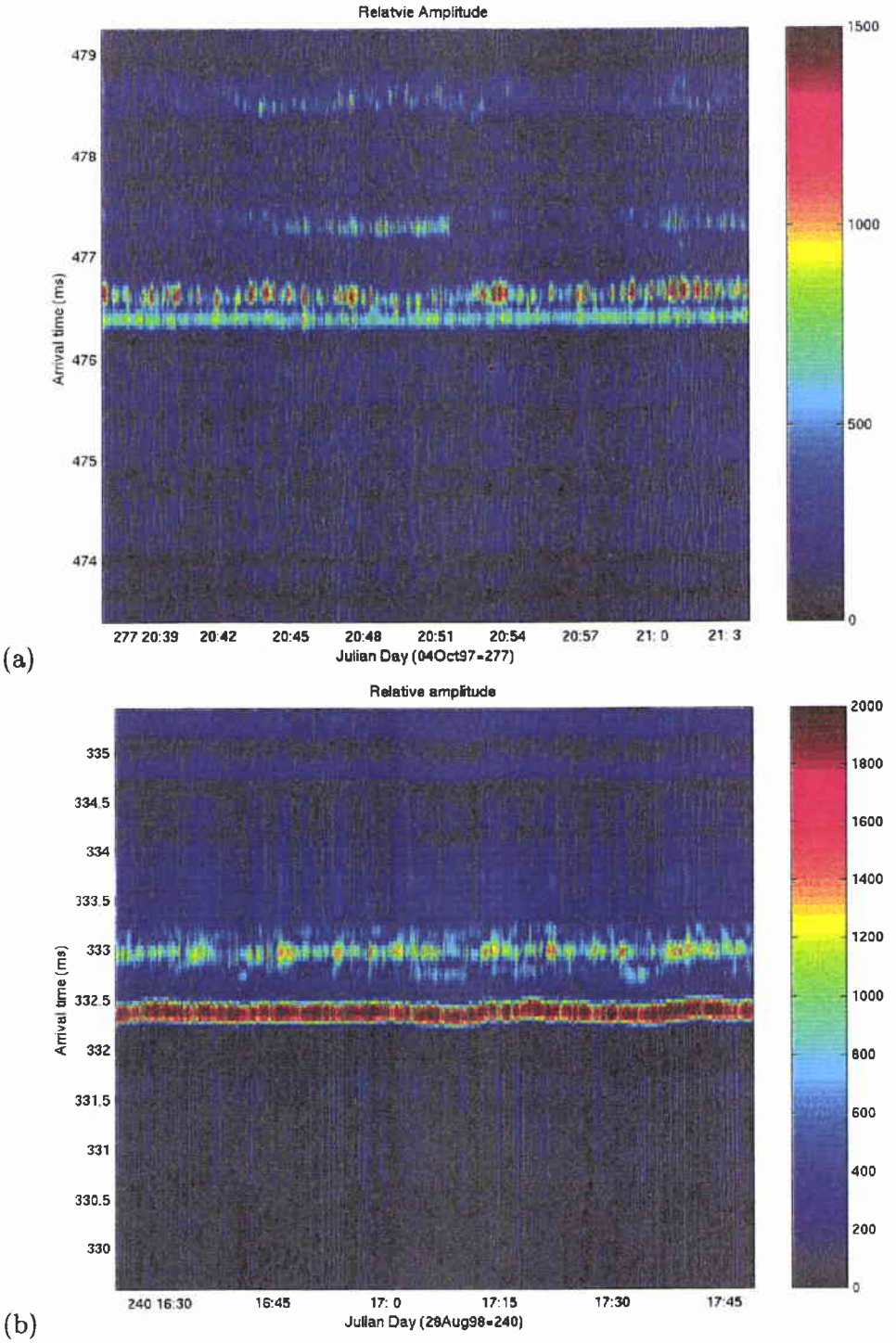

Figure 9 *(a) Relative amplitude as a function of arrival time and elapsed time for the upper layer system and (b) lower layer system.*

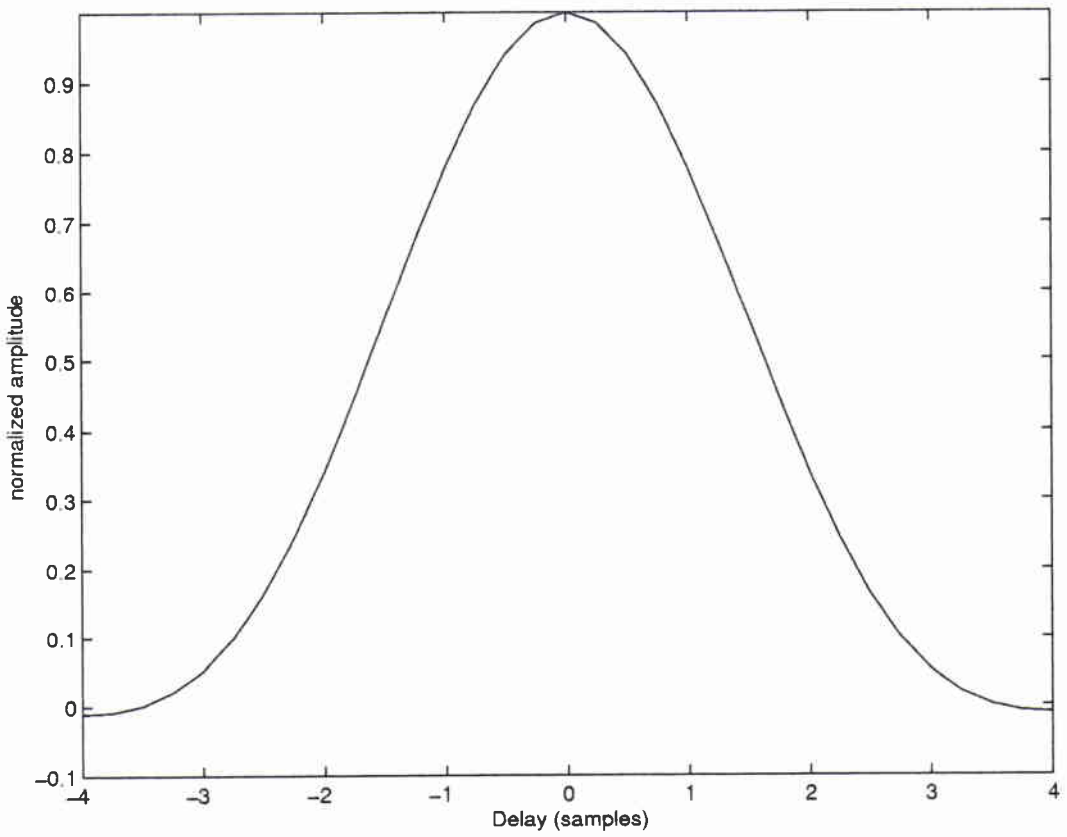

Figure 10 *Correlation of the received signal with a template of the transmitted pseudo random noise (PRN) code (3 samples = 1 bit = 120 μs).*

with respect to A and T. The function,

$$C(T) = \sum_t r(t)s(t-T) \tag{11}$$

is the cross correlation between the received and modelled signal and the function,

$$B(0) = \sum_t s(t-T)s(t-T), \tag{12}$$

is the auto correlation of the modelled signal. Minimizing Q implies that the second term on the right of (10) should be maximized with respect to the unknown variables. That is,

$$\text{maximize} \quad AC(T) - \frac{1}{2}A^2B(0) \quad \text{w.r.t. } A \text{ and } T. \tag{13}$$

Maximizing (13) with respect to A yields,

$$A = \frac{C(T)}{B(0)}. \tag{14}$$

Substituting (14) into (13) gives the following maximization problem,

$$\text{maximize} \quad \frac{1}{2}\frac{C(T)^2}{B(0)} \quad \text{w.r.t. } T. \tag{15}$$

Therefore, to determine the maximum likelihood estimate, (15) must first be maximized with respect to the arrival time. This equation is quadratic and is a function of one independent variable and so maximization occurs over a one-dimensional space. The algorithm used from MATLAB is based on the golden section search and parabolic interpolation. In order to find the arrival time that maximizes (15), a starting point must be given. For the very first transmission the starting point can be determined by peak detection; for subsequent transmissions the arrival time for the previous transmission can be used as a starting point. The minimization algorithm then converges quickly to the new arrival time that maximizes (15). These values are then used in (14) to obtain the amplitude estimate. The phase is then calculated by linear interpolation.

Windowing of the data is crucial. As the peak width is defined by $2\tau_p = 6$ samples say, then it is ideal to do the estimation over only 7 samples. This will involve adjusting the window with time so that the peak remains centered in the window. Hence a peak tracking routine is required. Some tests were carried out and it was found that a window centered on a running average of the time of arrival was ideal. Taking the center of the window on a specific time of arrival may cause the window to shift, thus including only part of the peak and causing problems. This windowing problem may arise because the time of arrival can be a noisy estimate.

The output from the maximum likelihood estimation algorithm is shown in Figure 11. The amplitude and phase are shown as a function of travel time in samples. The direct path is the first arrival. Superimposed on the amplitude data is the theoretical shaped curve having width of 3 samples/bit in blue and 4 samples/bit in red. The best fit in a least squares sense is with the theoretical curve having bit width of 4 samples even though the data are sampled at 3 samples/bit. Thus the correlation peak is wider than expected. A number of factors may cause the correlation curve to deviate from its theoretical shape since m-sequence codes are very sensitive. For example, if there is a problem with digitization such that extra samples are added or some samples are lost then correlation with the template will cause distortion in the peak resulting in lower SNR and a wider peak. Also, multipath interference can cause distortions to the signal arrival.

The phase of the direct arrival is determined by linear interpolation of the phase at the arrival time location as shown in Figure 11. The phase wraps around between $-\pi$ and π radians.

Figure 12 shows the amplitude, phase and arrival time as a function of elapsed time for signals propagating from Rumeli Hisari (west) to Anadolu Hisari (east)

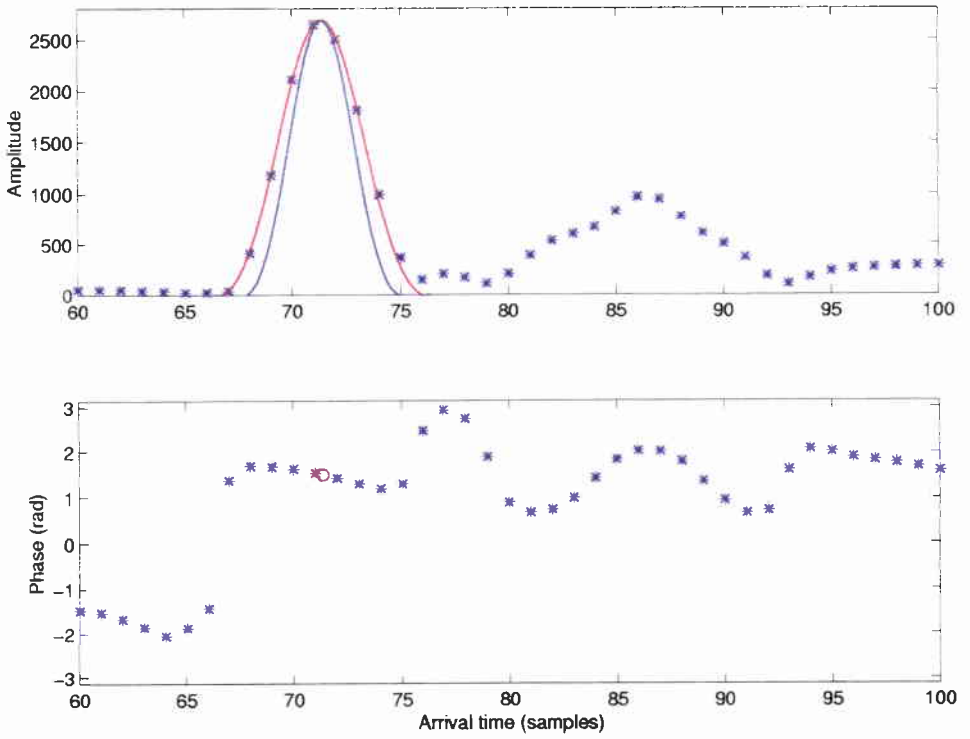

Figure 11 *(upper) Amplitude as a function of travel time together with the least squares fit of the theoretical curve (blue corresponds to 3 samples/bit and red corresponds to 4 samples/bit). (lower) Phase as a function of arrival time together with the linear interpolated phase at the arrival time location (red circle).*

and for signals propagating in the reciprocal direction using the lower layer system. Much high frequency variability exists in the amplitude measurement because of the turbulent nature of the flow. In fact, the amplitude shows similar variations for the forward and reciprocal direction. The phase in the forward direction shows jumps of $\pi/4$ and $\pi/2$ toward the negative direction. When these jumps wrap around they appear as positive jumps. The phase in the reciprocal direction show random jumps of an integral number of $\pi/4$. These jumps may be associated with a distorted master clock trigger signal used for analog to digital conversion. By the time the trigger signal travels down the cable to the subsurface units it becomes distorted. For the reciprocal direction the trigger travels down the 1400 m cross channel cable to the junction box and then down 400 m of cable to the subsurface unit and hence the phase and travel time are more noisy than in the forward direction.

Correcting the phase proved very difficult and thus it is concluded that it cannot be used to determine the turbulent nature of sound speed and current velocity on the total scattered signal. The mean travel time however, can be used to calculate the mean properties of the sound speed and current velocity. The amplitude can

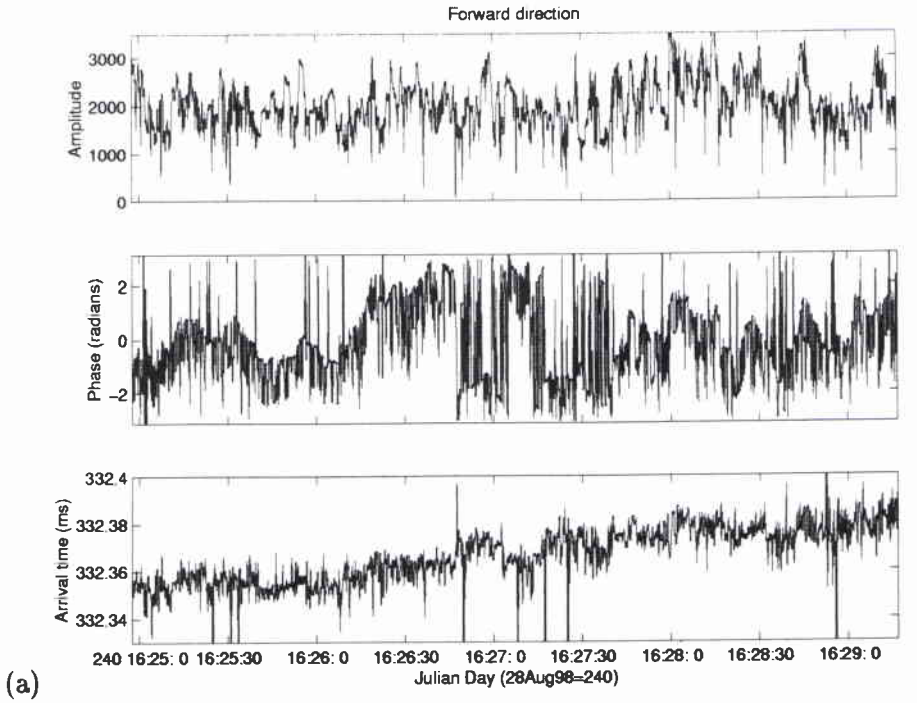

(a)

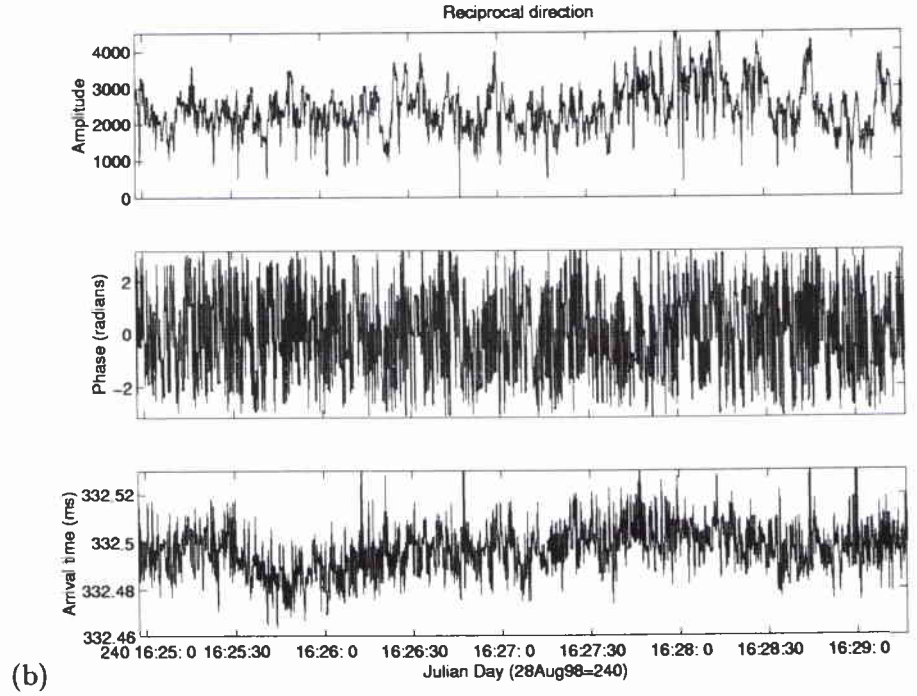

(b)

Figure 12 *Amplitude, phase and arrival time as a function of elapsed time for (a) the forward direction and (b) the reciprocal direction.*

be used to give a measure of the level of the effective refractive index fluctuations which is related to both the sound speed and current velocity variations.

6

Conclusions

We have summarised an approach to the use of high frequency acoustical propagation for the measurement of currents and water properties in coastal straits. The application discussed here is primarily for use over modest distances of a few km, which allows use of relatively high acoustical frequencies. However, the concept is applicable over greater distances provided a suitable sound channel exists. A distinguishing characteristic of the scintillation method is that the measurement is of flow perpendicular to the acoustical path. This differs for example from long range reciprocal tomography in the ocean, in which the measurement is restricted to the component along the path, although we also employ this same technique in the present implementation in order to achieve two orthogonal components of the current vector. Thus we exploit the finite decorrelation time of the spatially variable refractive field as it drifts through successive acoustic paths.

As the phase cannot be used as a sensitive measurement of the travel time, measurement of the sound speed and current velocity fluctuations to a precision of 1 $mm\ s^{-1}$ cannot be obtained. However, the mean properties can be determined from the mean arrival time. The amplitude fluctuations will give a measure of the turbulent levels but it cannot distinguish between sound speed (ie. temperature) effects and current velocity variability.

The practical implementation of the scintillation technique presents a number of engineering challenges. Real time processing is required to exploit high transmission rates together with the large bandwidth at relatively high frequencies. The design makes extensive use of modern digital signal processing technology.

7

Acknowledgements

The authors would like to make special thanks to the Department of Navigation Hydrography and Oceanography for providing all the necessary support for deployment and recovery procedures. We thank all captains and crew of Turkish Navy vessels involved in the deployment, recovery and redeployment. We make special thanks to Lt. Erhan Gezgin who put much effort in taking care of the logistics for the SIREN system especially with Istanbul traffic control. Many thanks to Piero Guerrini and Alessandro Brogini who provided the technical aspects for the deployment. Thanks to Tuncay Akal for his support in seeing this project through.

The development of acoustical scintillation technology has been sponsored throughout by the US Office of Naval Research, most recently under the program administered by Dr. Jeff Simmen together with funding from the Canadian Panel on Energy Research Development.

References

Crawford, G., Lataitis, R., and Clifford, S. (1990). Remote sensing of ocean flows by spatial filtering of acoustic scintillations: Theory. *Journal Acoustical Society America*, 88:442–453.

Curran, T., Lemon, D., and Ye, Z. (1994). Acoustic scintillation flowmeter: applications for a new environmental tool. *Journal Canadian Hydrographic Association*, 49:25–28.

Di Iorio, D. and Farmer, D. (1993). Observations of acoustical scintillations in Saanich Inlet. In *Oceans 1993 Proceedings, Engineering in Harmony with the Ocean*, October 18-21, Victoria, B.C. Canada.

Di Iorio, D. and Farmer, D. (1994). Path averaged turbulent dissipation measurements using high frequency acoustical scintillation analysis. *Journal Acoustical Society America*, 96:1056–1069.

Di Iorio, D. and Farmer, D. (1996). Two dimensional angle of arrival fluctuations. *Journal Acoustical Society America*, 100:814–824.

Di Iorio, D. and Farmer, D. (1998). Separation of current and sound speed in the effective refractive index for a turbulent environment using reciprocal acoustic transmission. *Journal Acoustical Society America*, 103:321–329.

Dixon, R. (1984). *Spread Spectrum Systems. A Wiley-Interscience Publication.* John Wiley and Sons, Toronto, 2nd edition.

Ehrenberg, J., Ewart, T., and Morris, R. (1978). Signal processing techniques for resolving individual pulses in a multipath signal. *Journal Acoustical Society America*, 63:1861–1865.

Farmer, D. and Clifford, S. (1986). Space-time acoustic scintillation analysis: A new technique for probing ocean flows. *IEEE Journal Oceanic Engineering*, 11:42–50.

Farmer, D., Clifford, S., and Verrall, J. (1985). Scintillation structure of a turbulent tidal flow. *Journal Geophysical Research*, 92:5369–5382.

Farmer, D. and Crawford, G. (1991). Remote sensing of ocean flows by spatial filtering of acoustic scintillations: Observations. *Journal Acoustical Society America*, 90:1582–1592.

Ishimaru, A. (1978). *Wave Propagation and Scattering in Random Media*, volume 2. Academic Press Inc.

Marsigli, L. F. (1681). Osservazioni intorno al Bosporo - Tracio overo canale di Constantinopoli. *Rappresente in Lettera alla Sacra Real Maesta' Christina Regina di Svezia, Roma.*

Menemenlis, D. (1994). Line-averaged measurement of velocity fine structure in the ocean using acoustical reciprocal transmission. *International Journal Remote Sensing*, 15:267–281.

Menemenlis, D. and Farmer, D. (1992). Acoustical measurements of current and vorticity beneath ice. *Journal Atmospheric Oceanic Technology*, 9:827–849.

Ünlüata, U., Oğuz, T., Latif, M., and Özsoy, E. (1990). On the physical oceanography of the Turkish Straits. In Pratt, L., editor, *The Physical Oceanography of Sea Straits*, pages 25–60. Kluwer Acad., Norwell, Mass.

Ye, Z., Curran, T., and Lemon, D. (1996). Fish detection by scintillation technique. *ICES Journal Marine Science*, 53:317–321.

Ye, Z. and Farmer, D. (1996). Acoustic scattering by fish in forward directin. *ICES Journal Marine Science*, 53:249–252.

Annex A
Data file formats

A.1 Scintillation data files

Ascii header format

The following is C code used to read the ascii header.

```
fscanf(fp,"Title is: %s\r\n",Title);
fscanf(fp,"Start Date is: %d/%d/%d\r\n",&mon,&day,&year);
fscanf(fp,"Start Time is: %d:%d:%d\r\n",&hour,&min,&sec);
fscanf(fp,"Ping Rate=%f(Hz)\r\n",&pRate);
fscanf(fp,"TxRx Delay=%f(ms)\r\n",&tDelay);
fscanf(fp,"Digitization Cycle=%f(us)\r\n",&mClk);
fscanf(fp,"Under_Sample_Factor=%d\r\n",&uSamp);
fscanf(fp,"Propagation Time=%f(ms)\r\n",&pTime);
fscanf(fp,"Master Sub_Window Size=%d(samples)\r\n",&MsSize);
fscanf(fp,"Slave Sub_Window Size=%d(samples)\r\n",&SsSize);
fscanf(fp,"Code ID: M1=%d,M2=%d,S1=%d,S2=%d\r\n",&c1,&c2,&c3,&c4);
fscanf(fp,"Code Length=%d\r\n",&cLength);
fscanf(fp,"Chip Width=%d\r\n",&cWidth);
fscanf(fp,"Number of Code=%d\r\n",&nCode);
fscanf(fp,"M_Tx Level(channel 0)=%d\r\n",&MU_Txlevel_0);
fscanf(fp,"M_Tx Level(channel 1)=%d\r\n",&MU_Txlevel_1);
fscanf(fp,"S_Tx Level(channel 0)=%d\r\n",&SU_Txlevel_0);
fscanf(fp,"S_Tx Level(channel 1)=%d\r\n",&SU_Txlevel_1);
fscanf(fp,"M_Rx Gain(channel 0)=%d\r\n",&MU_Rxgain_0);
fscanf(fp,"M_Rx Gain(channel 1)=%d\r\n",&MU_Rxgain_1);
fscanf(fp,"S_Rx Gain(channel 0)=%d\r\n",&SU_Rxgain_0);
fscanf(fp,"S_Rx Gain(channel 1)=%d\r\n",&SU_Rxgain_1);
fscanf(fp,"Data order is: %s\r\n4",&Order);
fscanf(fp,"WorkMode=%d,OnTime=%d,OffTime=%d\r\nn",&wmod,&ont,&offt);
```

binary data format

Immediately following the ascii header the binary data begins. From the master and slave sub_window size, each recorded record has length (2+8*MsSize+8*SsSize)

16-bit integers.

In each record, the first two short-integers make up the ping number.
d_in[1] is the higher 16-bit of the ping number
d_in[2] is the lower 16-bit of the ping number
Combine these two short-integers into a long integer, so
pingnumber = d_in[1]*65535 + d_in[2];

There are 8 channels of data in each record. Each channel includes real part and imaginary part put in interlace order. That is,
d_in[3],... d_in[2+2*MsSize] are channel M0S0 with
d_in[3],d_in[5],d_in[7], ... d_in(1+2*MsSize) quadrature data of M0S0
d_in[4],d_in[6],d_in[8], ... d_in(2+2*MsSize) inphase data of M0S0
d_in[3+2*MsSize],... d_in[2+4*MsSize],... are channel M0S1
d_in[3+4*MsSize],... d_in[2+6*MsSize],... are channel M1S0
d_in[3+6*MsSize],... d_in[2+8*MsSize],... are chennel M1S1
d_in[3+8*MsSize],... d_in[2+8*MsSzie+2*SsSize],... are channel S0M0
d_in[3+8*MsSize+2*SsSize],... d_in[2+8*MsSize+4*SsSize],... are channel S0M1
d_in[3+8*MsSize+4*SsSize],... d_in[2+8*MsSize+6*SsSize],... are channel S1M0
d_in[3+8*MsSize+6*SsSize],... d_in[2+8*MsSize+8*SsSize],... are channel S1M1

Channel M0S0 for example corresponds to Master receiver channel 0 listening to Slave transmission channel 0.

A.2 Environmental data files

This is ASCII data and has the following format,

```
MU::0051397153607H331.8X+00.26Y-05.59D010.699C31.930T+11.237#
```

MU::	Master Upper (Master Lower(ML), Slave Upper(SU), Slave Lower(SL))
0	Error Code (1, 2, 3)
05	Month
13	Day
97	Year
153607	hour, min, sec (hhmmss)
H331.8	331.8 degrees magnetic heading
X+00.26	00.26 tilt (+ up, - down)
Y-05.59	05.59 roll (+ clockwise, -counter clockwise)
D010.699	10.699 psi pressure

C31.930	31.930 mmho/cm conductivity
T+11.237	+11.237 degress celcius
#	checksum character

Report no. changed (Mar 2006): SM-354-UU

Document Data Sheet

Security Classification		Project No.
UNCLASSIFIED		033-5
Document Serial No.	**Date of Issue**	**Total Pages**
SM-354	February 1999	41 pp.

Author(s)

Di Iorio, D., Farmer, D.M., Cartier, W., Geng, X.

Title

Scintillation Instrument for Remote Environmental Analysis (SIREN)

Abstract

An acoustic propagation instrument is described that was developed to study ocean variability in the Strait of Istanbul (Bosporus). The scintillation instrument for remote environmental analysis (SIREN) was designed in modular form taking advantage of modern digital signal processing hardware and software so that continuous data can be collected at relatively high transmission rates and in reciprocal directions. The overall design and operation of the system proved to be very good except for a digitization triggering problem as a result of a distorted trigger signal because of cable lengths. This problem affected the measurement of the acoustic phase and hence the accuracy of ocean parameters for turbulence measurements. The amplitude however can be used as a measure of the total scattered signal due to turbulent sound speed and current velocity. The mean travel time gives mean ocean variability. The experimental period is summarized and the data processing techniques are described.

Keywords

Issuing Organization

North Atlantic Treaty Organization
SACLANT Undersea Research Centre
Viale San Bartolomeo 400, 19138 La Spezia, Italy

[From N. America: SACLANTCEN (New York) APO AE 09613]

Tel: +39 0187 527 361
Fax:+39 0187 524 600

E-mail: library@saclantc.nato.int